

Preparation of iron oxide nanoparticles supported on magnesium oxide for producing high-quality single-walled carbon nanotubes

Wei-Wen Liu¹, Azizan Aziz^{1*}, Siang-Piao Chai², Abdul Rahman Mohamed³, Ching-Thian Tye³

¹School of Materials and Mineral Resources Engineering, Engineering Campus, Universiti Sains Malaysia, 14300 Nibong Tebal, Seberang Perai Selatan, Malaysia

²School of Engineering, Monash University, Jalan Lagoon Selatan, 46150 Bandar Sunway, Selangor, Malaysia

³School of Chemical Engineering, Engineering Campus, Universiti Sains Malaysia, 14300 Nibong Tebal, Seberang Perai Selatan, Malaysia

Abstract: Fe₃O₄ nanoparticles with a narrow diameter distribution having an average diameter of 10.33 nm ± 2.99 nm (average diameter ± standard deviation) were prepared by a precipitation method. The Fe₃O₄ nanoparticles were supported on MgO by mixing the MgO nanopowder with the required amount of Fe₃O₄ nanoparticles in water under extensive sonication. Single-walled carbon nanotubes (SWCNTs) were synthesized by the chemical vapor deposition (CVD) of methane over the Fe₃O₄/MgO catalyst. Transmission electron microscopy showed that a large number of SWCNT bundles of nearly uniform diameter were produced by the CVD method. The average diameter of the produced SWCNTs was ca. 1.22 nm. Thermogravimetric analysis showed that the weight loss was approximately 19% by oxidation of carbon in the temperature range of 400–680 °C. The ratio of the intensity of the D-band to the G-band was 0.03, indicating that the SWCNTs were well-graphitized.

Key Words: Single-walled carbon nanotubes; Chemical vapor deposition; Electron microscopy; Raman spectroscopy

1 Introduction

The discovery of multiwalled carbon nanotubes (MWCNTs) in 1991^[1] and single-walled carbon nanotubes (SWCNTs) in 1993^[2] have attracted attention of many researchers. The excellent electrical conductivity properties of SWCNTs, in particular, can lead to the development of advanced electronic devices in near future. To permit the wide use of SWCNTs, it is essential to develop a production system that can synthesize SWCNTs in large quantity at low cost. However, both the arc-discharge and the laser ablation methods that are currently being used to prepare SWCNTs require extremely high temperatures and both the methods only produce a small amount of SWCNTs. In addition, these methods have difficulty in controlling the various growth conditions for synthesizing SWCNTs and thus are not suitable for large-scale production. Chemical vapor deposition (CVD) method has been developed to meet the requirement of a low-cost production for nanotubes, and also the controlled formation of carbon nanotubes (CNTs) could be achieved by CVD method.

It has been reported that the iron-based catalysts could selectively grow SWCNTs^[3–7], whereas cobalt- and nickel-based catalysts are more selective for the synthesis of

MWCNTs^[8–11]. The possibility to use Fe₃O₄ nanoparticles as a catalyst for CVD synthesis of MWCNTs^[12–13] and SWCNTs^[14–15] has been previously reported. These Fe₃O₄ nanoparticles were synthesized from various chemical and physical methods as reported^[16–18].

Recently, we reported that the synthesis of SWCNTs by the catalytic decomposition of methane can be achieved using the unreduced NiO/Al₂O₃ and Fe₂O₃/Al₂O₃ catalysts^[19–20]. However, the yield and the quality of the produced SWCNTs were significantly low. In this study, the synthesis of SWCNTs from catalytic decomposition of methane over Fe₃O₄/MgO was investigated. A precipitation method was then used to produce these Fe₃O₄ nanoparticles. The catalysts were prepared in a rotary evaporator to prevent the nanoparticles from being settled out from the dispersion over time. This allows the preparation of Fe₃O₄ nanoparticles with almost even diameter distribution. Surprisingly, an abundance of high-quality SWCNTs in form of bundles were grown over the Fe₃O₄/MgO catalyst.

2 Experimental

2.1 Preparation of catalyst

Homogeneous Fe₃O₄ nanoparticles were prepared in an

Received date: 21 November 2010; Revised date: 12 August 2011

*Corresponding author. E-mail: azizan@eng.usm.my

Copyright©2011, Institute of Coal Chemistry, Chinese Academy of Sciences. Published by Elsevier Limited. All rights reserved.

DOI: 10.1016/S1872-5805(11)60080-2

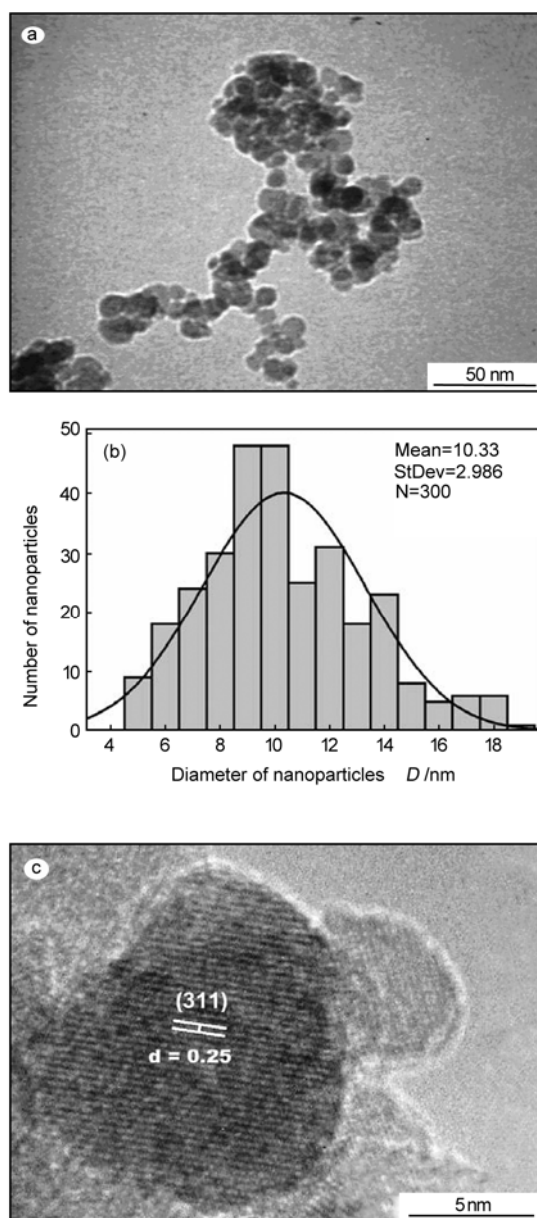
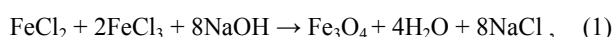


Fig.1 (a) Histogram showing the diameter distribution of Fe_3O_4 nanoparticles. (b) TEM image of Fe_3O_4 nanoparticles. (c) HRTEM image of Fe_3O_4 nanoparticles.

aqueous solution as shown in equation (1). The molar ratio of Fe(II) to Fe(III) was set at 0.5, and the pH was in a range of 11–12.



The aqueous solution was prepared by dissolving 4 mL of a 0.2 mol/L HCl solution, 0.69 g of FeCl_3 , and 0.25 g of FeCl_2 in 25 mL of purified, deoxygenated water. The water has been previously degassed by bubbling N_2 gas through it for 30 min while stirring gently. Subsequently, 250 mL of 1.2 mol/L NaOH solution was quickly added under vigorous stirring, instantly generating a black precipitate. The resulting black precipitate was isolated by centrifugation at 12 000 r/min, and the supernatant was removed from the precipitate by decantation. Purified, deoxygenated water was added to the precipitate, and the solution was again decanted after

centrifugation at 12 000 r/min. After repeating this procedure three times, 500 mL of 0.01 mol/L HCl solution was added to the precipitate, and the solution was stirred to neutralize the anionic charges on the nanoparticles. A sample was removed and then dried in an oven. The weight of the Fe_3O_4 nanoparticles was then used to calculate the amount of the MgO needed for preparing the catalyst with the desired composition. The mole ratio for Fe_3O_4 to MgO was set at 1:9. Catalysts were prepared by dispersing the MgO nanopowder in water with the required volume of Fe_3O_4 nanoparticles. The solution was then sonicated for 10 min and the water was removed using rotary evaporator. The dried catalyst was ground with a mortar and pestle to break up any agglomerates to produce very fine powders.

2.2 CNT synthesis

The synthesis of SWCNTs was carried out under atmospheric pressure in a quartz tube that was placed vertically in a stainless steel housing. To synthesize the SWCNTs, 0.2 g of catalyst were added to the middle of the reactor. The reactor was then heated in a tubular furnace to 900 °C in flowing N_2 (99.999% purity, supplied by Sitt Tatt Industrial Gases Sdn. Bhd.) at a flow rate of 40 mL/min. Subsequently, high-purity methane (99.999% purity, supplied by Malaysian Oxygen Bhd.) was mixed with N_2 at a ratio of volume 1:1 before introducing into the quartz reactor. The reaction was stopped after 30 min. The nanoparticle inside the furnace was then cooled to room temperature under nitrogen flow.

2.3 Characterization

The prepared Fe_3O_4 nanoparticles and the $\text{Fe}_3\text{O}_4/\text{MgO}$ catalysts were characterized using transmission electron microscope (TEM) (Philips CM12) and high-resolution TEM (HRTEM) (Philips FEI TECNAI 20). Energy-dispersive X-ray (EDX) spectra were also collected using the Philips FEI TECNAI 20. The structure and morphology of the synthesized CNTs were characterized using scanning electron microscope (SEM) (Supra 35VP-24-58) and TEM. Raman measurements were performed on the carbon samples using Raman spectroscopy (inVia Renishaw) at a wavelength of 633 nm with He-Ne laser excitation. X-ray diffraction (XRD) patterns of the fresh catalysts were characterized by Bruker AXS D8 Advance diffractometer using $\text{CuK}\alpha$ radiation and a graphite secondary beam monochromator. The intensity was measured by step scanning in a 2θ range of 10–90° with 0.034° steps and a measuring time of 2 s per point. The amount of deposited carbon was characterized using thermogravimetric analysis (TGA) (TA Instrument SDTQ600). The samples were heated in flowing air (100 mL/min) from 35 to 900 °C at a heating rate of 10 °C/min.

3 Results and discussion

3.1 Synthesis of Fe_3O_4 nanoparticles

Fig.1a shows the TEM image of the Fe_3O_4 nanoparticles,

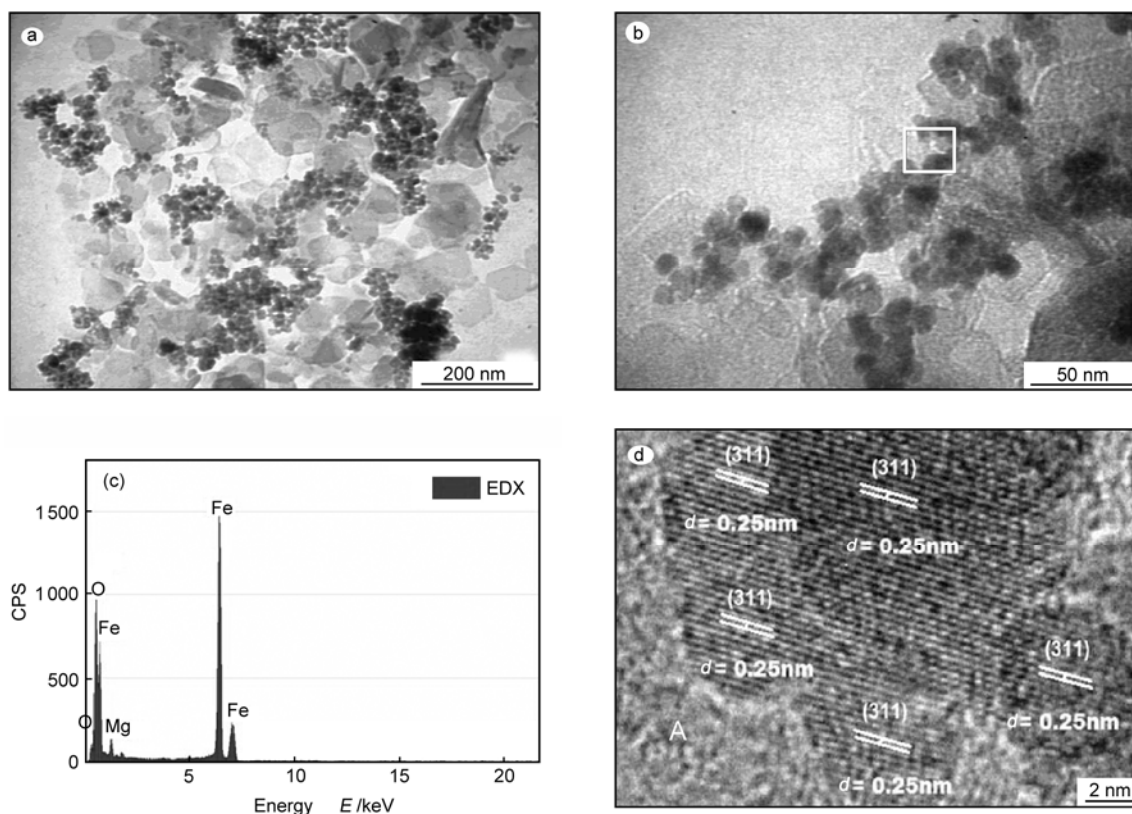


Fig.2 (a) Low-magnified and (b) high-magnified TEM images of Fe_3O_4 nanoparticles supported on MgO. (c) EDX analysis of the $\text{Fe}_3\text{O}_4/\text{MgO}$ catalyst. (d) HRTEM image of the $\text{Fe}_3\text{O}_4/\text{MgO}$ catalyst

which appeared to be nearly spherical shape. Approximately, 300 Fe_3O_4 nanoparticles were measured from their TEM images and the histogram was drawn as shown in Fig.1b. The average diameter of the Fe_3O_4 nanoparticles was 10.33 nm with a standard deviation of 2.99 nm. Fig.1c shows the high-resolution TEM (HRTEM) image of a Fe_3O_4 nanoparticle. The distance between two lattice planes of the crystallite was 0.25 nm, which is identical to the d-spacing of Fe_3O_4 from the standard diffraction of Fe_3O_4 (01-075-0449).

3.2 Preparation of Fe_3O_4 nanoparticles supported on MgO

Fig.2a shows that smaller particles (black color) were distributed over the larger particles (grey color). The element analysis of the small particles and the large particles were performed using EDX on the marked spots as shown in Fig. 2b. The EDX shows the presence of Fe, Mg, and O (Fig.2c). From the HRTEM image (Fig.2d), the measured distance between two lattice planes of the crystallite was 0.25 nm, which is corresponding to Fe_3O_4 (01-075-0449). It can be speculated from the EDX that the spot marked with A (Fig. 2d) was mainly MgO that demonstrated a strong interaction with Fe_3O_4 due to the high-surface basicity as compared with the Fe_3O_4 nanoparticles^[21]. These interactions can be described in terms of Lewis acid/base interactions between the metal oxide supports and the metal catalyst particles^[22]. With this strong interaction between the Fe_3O_4 nanoparticles and the MgO, the mobility of Fe_3O_4 nanoparticles on MgO surface was limited and the agglomeration of these nanoparticles was reduced^[23].

This was favorable to maintain the size distribution of the Fe_3O_4 nanoparticles for the synthesis of SWCNTs.

Fig.3 shows the powder XRD patterns of the freshly prepared Fe_3O_4 nanoparticles and the $\text{Fe}_3\text{O}_4/\text{MgO}$ catalyst. The representative peaks for Fe_3O_4 and MgO were denoted in the XRD spectra. In Fig.3a, several sharp peaks, corresponding to the standard diffraction of Fe_3O_4 (01-075-0449), were noted, indicating that the Fe_3O_4 sample is crystalline. Standard diffraction of MgO (00-045-0946) and $\text{Mg}(\text{OH})_2$ (00-001-1169) were labeled in blue and green, respectively, in Fig. 3b. The formation of $\text{Mg}(\text{OH})_2$ phases was due to the high moisture content of the catalyst because of the short drying time (20 min) by the rotary evaporator at 80 °C. As shown in Fig. 3b, the intensity of the Fe_3O_4 peaks remained the same after mixing with the MgO support.

3.3 Synthesis of CNTs

Fig.4 shows the SEM images of the as-prepared CNTs. CNTs were observed on the surface of the catalyst (Fig. 4a). At a closer observation, these CNTs were formed abundantly all over the catalyst surface (Fig. 4b). The SEM discloses that well-formed CNTs were produced by the $\text{Fe}_3\text{O}_4/\text{MgO}$ catalyst.

Fig.5a shows the morphology of the CNTs generated at 900 °C from methane decomposition over the $\text{Fe}_3\text{O}_4/\text{MgO}$ catalyst. It was observed that the carbon deposits appeared in the form of SWCNT bundles with the bundle diameters ranging from 10 to 20 nm. The bundles comprised more than 10 SWCNTs with individual nanotube diameters in the range of

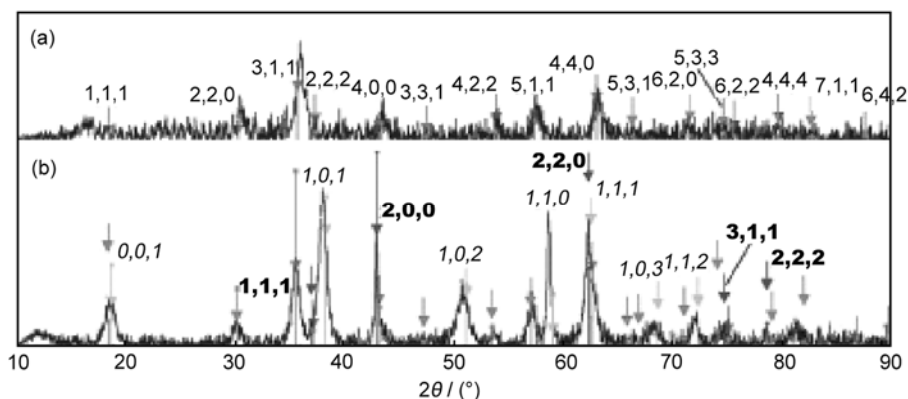


Fig.3 XRD patterns of (a) Fe_3O_4 nanoparticles (b) the $\text{Fe}_3\text{O}_4/\text{MgO}$ catalyst, (1,1,1): 01-075-0449(A)-Magnetite- Fe_3O_4 ; and (b) the $\text{Fe}_3\text{O}_4/\text{MgO}$ catalyst, (1,1,1): 00-045-0946 (*)-Periclase, syn-MgO, (1,1,1): 00-001-1169 (D)-Brucite- $\text{Mg}(\text{OH})_2$

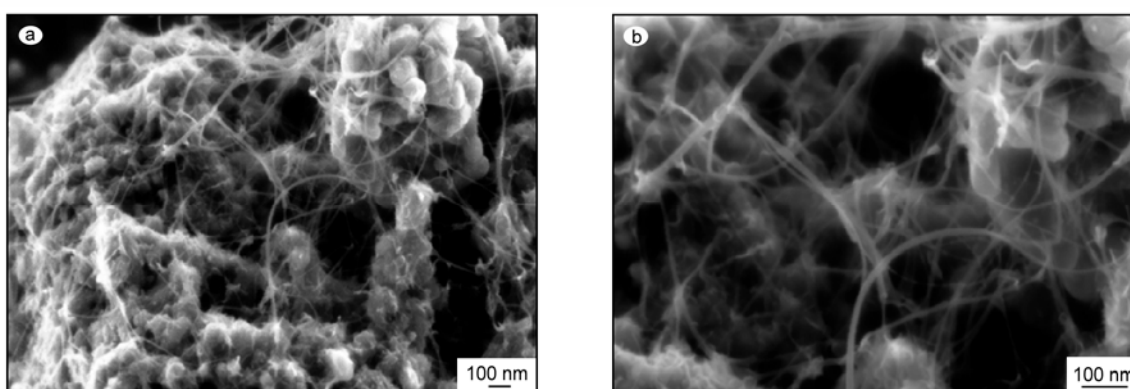


Fig.4 (a) Low-magnified and (b) high-magnified SEM images of the $\text{Fe}_3\text{O}_4/\text{MgO}$ catalyst after methane decomposition

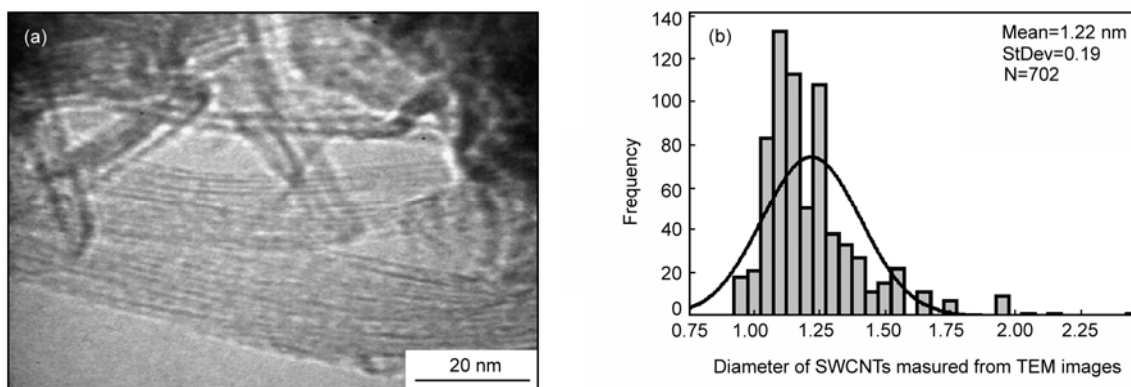


Fig.5 (a) TEM image of SWCNT bundles. (b) Diameter distributions of the SWCNTs

0.7-1.9 nm. It was found that occasionally SWCNTs appeared in an isolated form. However, they were most often packed together to form bundles due to the van der Waals interaction^[2]. The histogram of the nanotube diameters measured from the TEM images are shown in Fig.5b. The diameters of the CNTs were in a range of 0.90-2.10 nm. The average diameter was 1.22 nm with a standard deviation of 0.19 nm.

Raman analysis was performed to verify the presence of SWCNTs in the carbon samples. The resulting spectrum is shown in Fig.6. There were two characteristic peaks found in

the Raman spectrum at 1350 cm^{-1} and 1595 cm^{-1} , corresponding to the D- and G-bands, respectively. While the G-band is associated with the high degree of order in sp^2 -bonded carbon materials, the D-band is associated with disorder^[24]. A common measure of the quality of a nanotube sample is the ratio of the intensity of the D-band to the G-band (I_D/I_G)^[25-26]. Pure, defect-free SWCNTs have low I_D/I_G ratios. In this study, the calculated I_D/I_G was 0.03, indicating that the well-graphitized SWCNTs were grown.

The peaks at low wave number, i.e. $< 350\text{ cm}^{-1}$ (shown in Fig.7b), are called the radial breathing mode (RBM)^[27]. The

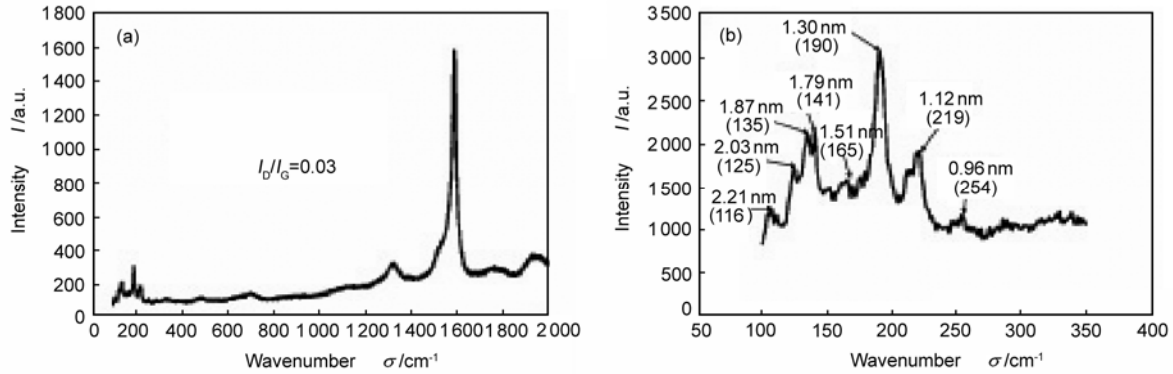


Fig.6 (a) Raman spectrum of SWCNTs. (b) The low-frequency region of Raman spectrum for the SWCNTs

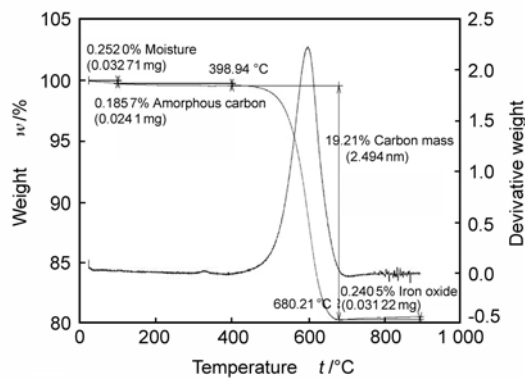


Fig.7 Thermal analysis of carbon sample

presence of RBM peaks is evidence that the sample contained SWCNTs. The frequency of the RBM is inversely proportional to the diameter of the nanotube from which it arises. It has been found empirically that the diameter of the tube (d_t /nm) can relate to the frequency of RBM (ω_{RBM}) by $\omega_{\text{RBM}} = A/d_t + B$, where $A = 234 \text{ cm}^{-1}$, $B = 10 \text{ cm}^{-1}$, and d_t = diameter of SWCNTs in nanometer^[28]. The results showed that the calculated diameters of SWCNTs were in a range of 0.96–2.21 nm, and it is in good agreement with the diameters measured from the TEM images. It is important to note that a single significant peak with a high intensity at Raman shift 190 cm^{-1} was observed. This peak implies that most of the produced SWCNTs were almost uniform in a diameter, i.e. ca. 1.30 nm, and this diameter was close to the average diameter presented in the histogram (Fig.5b).

TGA was used to determine the percentage yield of the carbon deposit. In Fig.7, the TGA shows the weight loss due to the oxidation of carbon at temperature range of 400–680 °C. The carbon content of the catalyst was calculated as $100 \times (m_1 - m_2)/m_1$, where m_1 and m_2 are the weights of the sample before and after the carbon oxidation, respectively. The calculated carbon content was 19%. The content of amorphous carbon was approximately 0.19%, a very low value as shown by the small bump appearing at 325 °C (Fig.7). The sample contained 0.25% moisture.

3.4 Growth mechanism of SWCNTs

The formation of SWCNTs by the $\text{Fe}_3\text{O}_4/\text{MgO}$ catalyst could be attributed to the strong metal interaction between the Fe_3O_4 nanoparticles and the MgO ^[22]. We believe that this strong interaction restricted the mobility of Fe_3O_4 nanoparticles during the CVD, thus preventing the extensive agglomeration of Fe_3O_4 nanoparticles at high temperature to form larger sized clusters. The growth mechanism can be explained using the vapor-liquid-solid model^[29]. At the initial stage of the catalytic reaction, methane was passed over the surface of the $\text{Fe}_3\text{O}_4/\text{MgO}$ catalyst and the methane was catalytically decomposed into carbon and hydrogen. The hydrogen acted as a reducing agent in reducing the Fe_3O_4 nanoparticles to Fe. This was followed by the diffusion of carbon atoms into the Fe, forming iron carbide in a cementite (Fe_3C) form^[30]. When the metal was supersaturated, carbon precipitated out of the iron carbide surface to form SWCNTs.

4 Conclusion

In this study, we demonstrated that Fe_3O_4 nanoparticles prepared by precipitation method were effective in synthesizing SWCNTs in a bundle form. The prepared Fe_3O_4 nanoparticles were small and nearly uniform in diameter. The quality of the SWCNTs produced by the MgO -supported Fe_3O_4 catalyst was verified by the Raman analysis. The low I_D/I_G ratio of 0.03 shows that the synthesized SWCNTs were well-graphitized. The single peak appearing at 190 cm^{-1} in the Raman spectrum indicates that SWCNTs with the diameter of ca. 1.30 nm appeared in majority. TGA analysis was further carried out to determine the carbon content of the catalyst after the reaction. The weight loss of 19% was observed, and the catalyst sample contained a very small amount of amorphous carbon as revealed by the TGA.

Acknowledgments

We gratefully acknowledge the financial support provided by the Universiti Sains Malaysia under Fundamental Research Grant Scheme (FRGS) (Project: A/C No. 6071002), Research University Grant (RU) (Project: A/C No. 814004),

and Skim Penyelidikan Siswazah Universiti Penyelidikan (USM-RU-PRGS) (Project: A/C No. 8042015) and USM Fellowship.

References

- [1] Iijima S. Helical microtubules of graphitic carbon[J]. *Nature*, 1991, 354(6348): 56-58.
- [2] Iijima S, Ichihashi T. Single-shell carbon nanotubes of 1-nm diameter[J]. *Nature*, 1993, 363: 603-605.
- [3] Cheng H M, Li F, Su G, et al. Large-scale and low-cost synthesis of single-walled carbon nanotubes by the catalytic pyrolysis of hydrocarbons[J]. *Applied Physics Letters*, 1998, 72(25): 3282-3284.
- [4] Li Y, Kim W, Zhang Y, et al. Growth of single-walled carbon nanotubes from discrete catalytic nanoparticles of various sizes[J]. *The Journal of Physical Chemistry B*, 2001, 105 (46): 11424-11431.
- [5] Cheung C L, Kurtz A, Park H, et al. Diameter-controlled synthesis of carbon nanotubes[J]. *The Journal of Physical Chemistry B*, 2002, 106 (10): 2429-2433.
- [6] Nikolaev P, Bronikowski M J, Bradley R K, et al. Gas-phase catalytic growth of single-walled carbon nanotubes from carbon monoxide[J]. *Chemical Physics Letters*, 1999, 313 (1-2): 91-97.
- [7] Zhu S, Su C H, Cochrane J C, et al. Growth orientation of carbon nanotubes by thermal chemical vapor deposition[J]. *Journal of Crystal Growth*, 2002, 234 (2-3): 584-588.
- [8] Ivanov V, Nagy J B, Lambin P, et al. The study of carbon nanotubes produced by catalytic method[J]. *Chemical Physics Letters*, 1994, 223 (4): 329-335.
- [9] Hernadi K, Fonseca A, Nagy J B, et al. Catalytic synthesis of carbon nanotubes using zeolite support[J]. *Zeolites*, 1996, 17 (5-6): 416-423.
- [10] Ago H, Komatsu T, Ohshima S, et al. Dispersion of metal nanoparticles for aligned carbon nanotube arrays[J]. *Applied Physics Letters*, 2000, 77 (1): 79-81.
- [11] Satishkumar B C, Govindaraj A, Sen R, et al. Single-walled nanotubes by the pyrolysis of acetylene-organometallic mixtures[J]. *Chemical Physics Letters*, 1998, 293(1-2): 47-52.
- [12] Li W Z, Xie S S, Qian L X, et al. large-scale synthesis of aligned carbon nanotubes[J]. *Science*, 1996, 274(5293): 1701-1703.
- [13] Xie S S, Chang B H, Li W Z, et al. Synthesis and characterization of aligned carbon nanotube arrays[J]. *Advanced Materials*, 1999, 11(13): 1135-1138.
- [14] Fu Q, Reed L, Liu J, et al. Characterization of single-walled carbon nanotubes synthesized using iron and cobalt nanoparticles derived from self-assembled diblock copolymer micelles[J]. *Applied Organometallic Chemistry*, 2010, 24(8): 569-572.
- [15] Zhang Y, Li Y, Kim W, et al. Imaging as-grown single-walled carbon nanotubes originated from isolated catalytic nanoparticles[J]. *Applied Physics A: Materials Science and Processing*, 2002, 74(3): 325-328.
- [16] Ahmadi T S, Wang Z L, Green T C, et al. Shape-controlled synthesis of colloidal platinum nanoparticles[J]. *Science*, 1996, 272(5270): 1924-1925.
- [17] Andres R P, Bielefeld J D, Henderson J I, et al. Self-assembly of a two-dimensional superlattice of molecularly linked metal clusters[J]. *Science*, 1996, 273(5282): 1690-1693.
- [18] Zach M P, Penner R M. Nanocrystalline nickel nanoparticles[J]. *Advanced Materials*, 2000, 12(12): 878-883.
- [19] Chai S P, Zein S H S, Mohamed A R. Moderate temperature synthesis of single-walled carbon nanotubes on alumina supported nickel oxide catalyst[J]. *Materials Letters*, 2007, 61(16): 3519-3521.
- [20] Tan S M, Chai S P, Liu W W, et al. Effects of FeOx, CoOx, and NiO catalysts and calcination temperatures on the synthesis of single-walled carbon nanotubes through chemical vapor deposition of methane[J]. *Journal of Alloys and Compounds*, 2009, 477(1-2): 785-788.
- [21] Sun C, Berg J C. A review of the different techniques for solid surface acid-base characterization[J]. *Advances in Colloid and Interface Science*, 2003, 105(1-3): 151-175.
- [22] Dupuis A C. The catalyst in the CCVD of carbon nanotubes-a review[J]. *Progress in Materials Science*, 2005, 50 (8): 929-961.
- [23] Moisala A, Nasibulin A G, Kauppinen E I. The role of metal nanoparticles in the catalytic production of single-walled carbon nanotubes-A review[J]. *Journal of Physics Condensed Matter*, 2003, 15(42).
- [24] Pimenta M A, Jorio A, Brown S D M, et al. Diameter dependence of the Raman D-band in isolated single-wall carbon nanotubes[J]. *Physical Review B-Condensed Matter and Materials Physics*, 2001, 64(4): 414011-414014.
- [25] Qian W, Liu T, Wei F, et al. Quantitative Raman characterization of the mixed samples of the single and multi-wall carbon nanotubes [J]. *Carbon*, 2003, 41 (9): 1851-1854.
- [26] Athalin H, Lefrant S. A correlated method for quantifying mixed and dispersed carbon nanotubes: Analysis of the Raman band intensities and evidence of wavenumber shift[J]. *Journal of Raman Spectroscopy*, 2005, 36 (5): 400-408.
- [27] Dresselhaus M S, Dresselhaus G, Saito R, et al. Raman spectroscopy of carbon nanotubes[J]. *Physics Reports*, 2005, 409 (2): 47-99.
- [28] Dresselhaus M S, Dresselhaus G, Jorio A, et al. Single nanotube Raman spectroscopy[J]. *Accounts of Chemical Research*, 2002, 35 (12): 1070-1078.
- [29] Baker R T K, Harris P S, Thomas R B, et al. Formation of filamentous carbon from iron, cobalt and chromium catalyzed decomposition of acetylene[J]. *Journal of Catalysis*, 1973, 30 (1): 86-95.